

Chapter 20

Large Eddy Simulation of Wind Farm Aerodynamics with Energy-Conserving Schemes

Dhruv Mehta

Abstract In order to truly realise the potential of wind power, it is vital to understand the aerodynamic losses over a wind farm. The current chapter highlights the importance of aerodynamic analysis of offshore wind farms, and presents a summarized review of Large Eddy Simulation literature. Furthermore, the chapter presents the objectives of the current research and concludes with a case study.

20.1 Introduction

This chapter presents a study on the Large Eddy Simulation of wind farm aerodynamics. Wind farm aerodynamics (WFA) deals with the interaction between wind turbine wakes and the atmospheric boundary layer (ABL), as they develop across the length of the wind farm. At times, the wakes also interact with each other and with other wind turbines (Mehta et al. 2014).

The study of WFA is crucial as it provides insight into the air flow through a wind farm, which eventually provides the energy that is converted into electricity by wind turbines. Therefore, one can assess the power produced by a wind farm by aerodynamically analysing the flow through the farm. The study of WFA requires aerodynamic data, which is generally gathered through meteorological masts in existing wind farms.

With the apparatus placed on these masts, we can measure the velocity and turbulence intensity (TI)—albeit at only a single point. In case the apparatus is an array of instruments, one may be able to measure the velocity (and TI) at more than a single point. Nonetheless, even in the best cases, the aerodynamic data for a few points on a wind farm is not enough to assess the power produced by the wind farm. Further, the erratic nature of the atmosphere makes it hard to relate the measured velocity (or TI) to its cause. For example, one cannot be certain whether

D. Mehta (✉)

Wind Energy Research Institute (DUWIND), Delft University, Kluyverweg 1, 2629 HS Delft, Netherlands

Energy Research Centre of the Netherlands (ECN), Westerduinweg 3, 1755 LE Petten, Netherlands

e-mail: d.mehta@tudelft.nl

the measured velocity (or TI) is from a single turbine’s wake, or due to a sudden gust through the farm etc. Thus, for a complete insight, it is important to complement experimental data with numerical data from simulations.

20.2 Simulation

To simulate the flow through a wind farm, one must numerically resolve the various eddies within the air flow. These eddies represent the different scales of turbulence. For a high Reynolds number flow, these eddies can be of various sizes (Pope 2000). In case of a wind farm, this difference in eddy sizes can be between a few millimetres corresponding to boundary layer on a turbine’s blade, and a kilometre corresponding to the height of the boundary layer. When the energy of these scales is plotted against their size, one obtains the energy spectrum as shown in Fig. 20.1.

The largest scales are the energy-containing integral range and the smallest ones are the dissipative, Kolmogorov scales (Tennekes and Lumley 1972). In between lies the inertial range. On a wind farm, these scales are about a few centimetres in size.

It is computationally impossible (with today’s resources) to resolve all these scales feasibly. Therefore, the wisest approach would be to numerically resolve only the large energy containing scales (and a part of inertial range), to gain insight into WFA. This approach is known as Large Eddy Simulation (LES); an example of

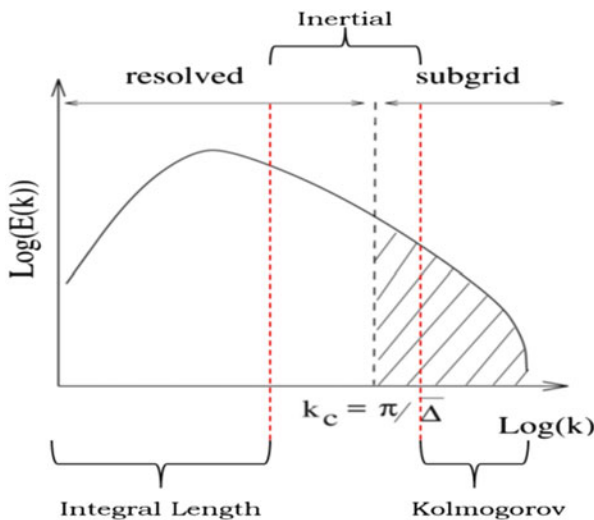


Fig. 20.1 The energy of the various eddies (y-axis) in a flow, plotted against their size (x-axis)

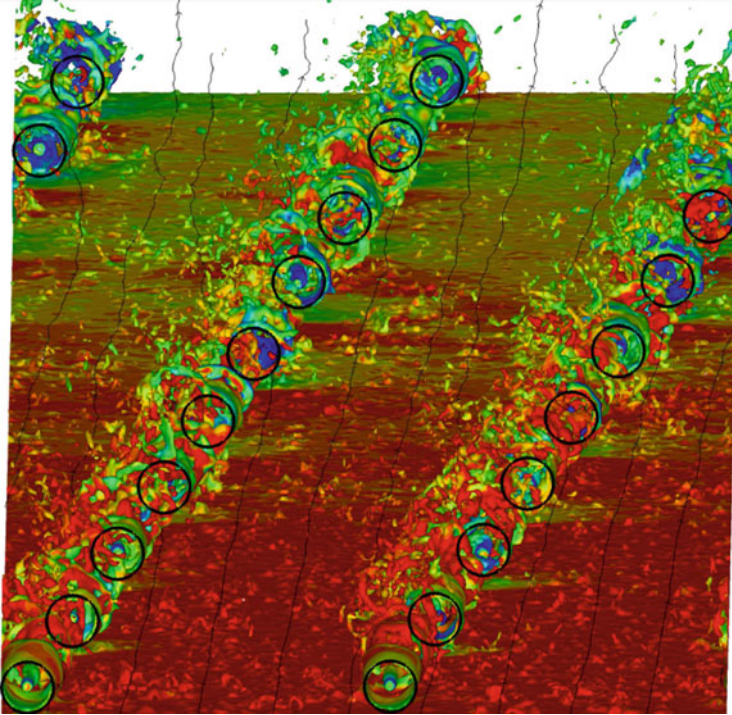


Fig. 20.2 Large Eddy Simulation of the Horns Rev wind farm [Source: Ivanel (2009)]

LES is shown in Fig. 20.2. As shown in Fig. 20.1, the scales that are numerically calculated are called the ‘resolved scales’ and the rest are known as the ‘subgrid scales’. The latter are numerically modelled with a subgrid scale (SGS) model.

20.3 Literature Review

A comprehensive literature review on LES was conducted by Mehta et al. (2014). We summarize the key points below:

- Wind farms simulations have been performed predominantly with eddy-viscosity models. Even the simple Smagorinsky’s model is sufficient for qualitative analyses of wind farm aerodynamics. But for accuracy, researchers must rely on more advanced SGS models.
- With proper ABL modelling, LES can help assess the performance of wind farms in off-design conditions like non-neutral ABLs and gusts. Effective coupling with aeroelastic codes could provide great insight into turbine loading in such situations.

- Wind farm simulations rely on accurate wake-ABL interaction, which is possible only with a correct ABL model. This is of great consequence for simulating large wind farms on which the ABL evolves into a wind turbine-ABL. Generating a synthetic ABL requires lesser computational effort than precursor simulations with LES, but lacks the statistical correlations that exist in a physical ABL.
- Using the Scale Dependent Dynamic model with Lagrangian averaging generates an ABL that is accurate enough for wind farm simulations, but is computationally expensive. Nonetheless, it retains its precision even on coarse grids making it suitable for LES.
- From simulations of the Horns Rev wind farm, it is apparent that the performance of engineering models is comparable to that of certain LES codes, as far as generating averaged statistics. When done with accurate ABL modelling and with advanced SGS models, on relatively refined grids, LES delivers a substantially better performance.
- LES data can be utilised to enhance simple engineering models to retain computational efficiency but ensuring better accuracy.
- Numerical schemes for LES must ensure zero numerical dissipation for high accuracy. Pseudo-spectral and Energy-Conserving spatial discretisation schemes are useful in this regard; the latter however requires a higher-order formulation to be as accurate as the former. Additionally, energy-conserving time integration with zero dissipation would help speed up computations, but requires further modifications to avert loss in accuracy and stability.
- A stress-free upper boundary is most appropriate for wind farm simulations. Periodic boundaries required by spectral schemes can be avoided with Energy-Conserving schemes, which are however not as accurate as the former.
- SGS models have been compared in terms of their ability to simulate the ABL. It is clear that above beyond a certain resolution, the effect of the SGS model on ABL is nullified and even a simple model is sufficient for an ABL simulation. However, such a conclusion with regard to wind farm simulations is yet to be drawn.

Concerning LES, it is certain that no SGS model is complete and their efficacy is situation-dependent. Smagorinsky's model and its derivatives are popular as they are easily implementable and capable of producing good data on wind farm aerodynamics, despite their assumptions lacking conclusive evidence. Regarding coarse grids, it would be wise to develop numerical schemes instead of relying on excess computational power. LES codes cannot count on upwind schemes of stability because the numerical dissipation will dampen the resolved scales, more so on coarse grids. High-order spectral methods are thus common in LES but are computationally expensive. On the other hand, Energy-conserving schemes are free from numerical dissipation and permit the use of non-periodic boundaries, but require further investigation at this stage.

In terms of boundary conditions, Monin-Obukov's (Panofsky and Dutton 1984) approach remains the only option for modelling the ABL, despite being deemed unsuitable for LES. Lately, research has been focussed on developing a more appropriate technique that could be adapted for inhomogeneous terrains, but experiments would be more instrumental in enhancing the existing approach.

20.4 Power Losses and Observations

Figure 20.3 shows the power generated by the various rows of wind turbines simulated as shown in Fig. 20.2. It can be observed that the power generation is the highest for turbines in the front row, which is exposed directly to the freestream ABL flow. However, turbines within this row generate a wake, which develops with downstream distance and interacts, in the case of Horns Rev, within downstream turbines.

Therefore, there is a sudden decrease in power generation by the second row. This is due to the reduced velocity in the wake. However, a wake not only bears a reduced velocity but also a higher turbulence intensity. This fact has been confirmed experimentally by Chamorro and Porté-Agel (2011) and numerically through LES by Stevens et al. (2013).

This increased turbulence promotes the mixing of the slower wake with the faster freestream ABL flow, leading to the reduction of the velocity deficit in the wake and increased velocity. This is the reason why the second row (Horns Rev,

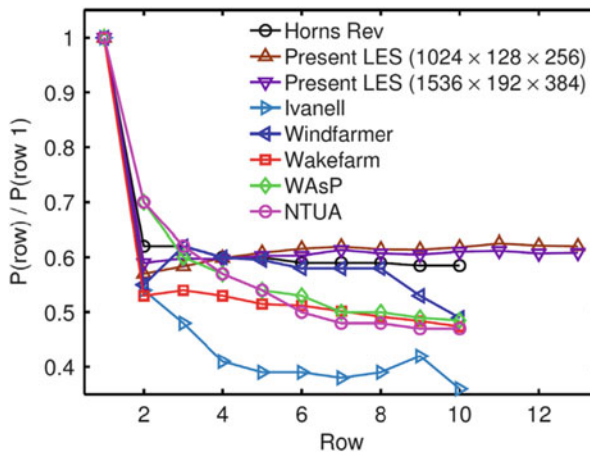


Fig. 20.3 The power output on the Horns-Rev wind farm predicted by an LES codes (present LES, and Ivallell (2009)) and various engineering models, adapted from Stevens et al. (2013). The power output on the y-axis has been normalised by the power output of the turbines in the first row. One notices the discrepancy between LES and simple engineering models

black line in Fig. 20.3), generates the highest power amongst all downstream rows. Further, the increased turbulence reaches a peak value after the wake from the first turbine interacts with the second turbine, leading to a slower wake; thus, after one wake-turbine interaction. At times, this could happen after two such wake-turbine interactions, in case the inflow turbulence is low (Mehta et al. 2014).

Once, the wake generated turbulence reaches its peak value, the recovery of the reduced velocity in the wake also reaches its limit. Therefore, after one or two wake-turbine interactions, the wake does not recover much, as a result, one notices a decline in power production across the rows on a wind farm. Nevertheless, the decrease is not steep as compared to the one noticed within the first two rows. The fact that the added turbulence has reached a steady peak value, ensures that the wake recovers after every wake-turbine interaction, to a value that is more or less similar to the inflow value. In effect, beyond the second or third row, the horizontal flow is fully developed, leading a similar power prediction as seen in Fig. 20.3 (Calaf et al. 2010).

Figure 20.3 also compares the data from LES and engineering models. These models are very simple and built upon the simplification of the flow phenomena. As a result, these models are fast and computationally efficient but not very accurate. Further, their accuracy is mostly related to the prediction of the average power output over a range of wind directions, and not for a particular inflow direction, which requires the application of LES (Barthelmie et al. 2009).

20.5 Research Objectives

The current research involves three phases:

- Implementing an SGS model in the Energy-Conserving Navier-Stokes (ECNS) code.
- Analysing energy-conserving (EC) spatial discretisation and EC time integration in terms of accuracy and efficiency.
- Validating the combination of the ECNS and the chosen SGS model for wind farm simulations.

20.6 Tests and Results

The following are the tests conducted, the results obtained and the conclusions drawn.

20.6.1 EC Time Integration

EC time integration available within the ECNS code is unconditionally stable for any time step. Further, it introduces no numerical dissipation during the simulation (Sanderse 2013). However, according to the literature, most existing LES codes would rely on non-EC time integration.

We therefore, used the case of decaying isotropic homogeneous turbulence, to assess whether an EC time integration scheme offers any advantage, in terms of accuracy. We observed that an implicit EC time scheme (4th order accurate), has a lower global error than a 4th order accurate, non-EC explicit time scheme. This error corresponds directly to the numerical dissipation (Fig. 20.4).

However, as shown in Fig. 20.4, the computational time required by the implicit EC time schemes, are much larger than those required by the explicit non-EC schemes. This disproportionality is such that, one is better off using a non-EC explicit time integration scheme (as done by existing LES codes) with a smaller time step, as opposed to an implicit EC scheme.

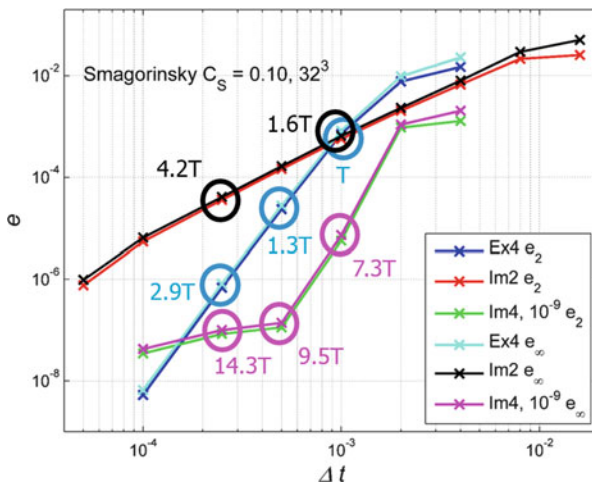


Fig. 20.4 A plot of the error vs. the time step use with three time integration methods: Ex4, explicit 4th order non-EC Runge-Kutta scheme; Im2, implicit 2nd order EC Gauss scheme and Im4, implicit 4th order EC Gauss scheme. T is the computational time take by Ex4 at a time step of 0.001 s

20.6.2 EC Spatial Discretisation

EC spatial discretisation done on a Cartesian staggered grid, is dissipation free for any grid size (Sanderson 2013). However, the scheme itself, is essentially a simple central difference scheme (Perić and Ferziger 2002).

We checked if using an EC spatial discretisation on a Cartesian staggered grid, is the same as using a simple central difference on a collocated Cartesian grid. Using a series of tests on inviscid vortices, we noticed that both the schemes are numerically alike. By extension, the absence of numerical dissipation in either scheme, reduces the grid dependence in tuning the Smagorinsky SGS model chosen for the ECNS (Fig. 20.5).

Therefore, we were able to tune the Smagorinsky model in the ECNS, to a value of the Smagorinsky constant, $C_S = 0.12$. Over a range of grid resolutions, this value of the Smagorinsky constant was reasonable enough to predict the behaviour of the large energy-containing scales, correctly.

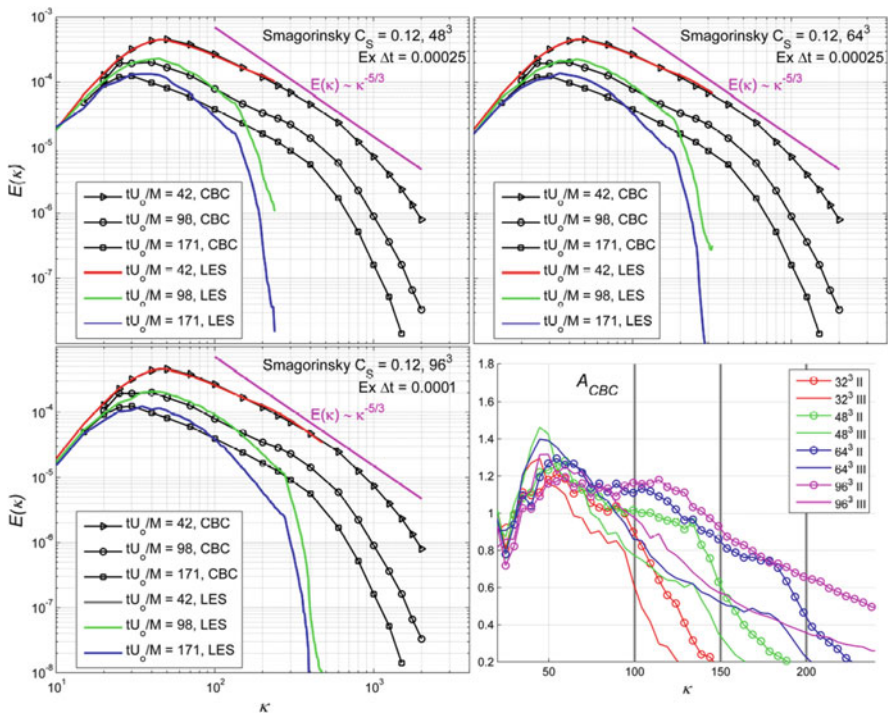


Fig. 20.5 Clockwise from *top-left*: the energy spectra obtained through experiments (Comté-Bellot and Corrsin 1971) compared against results with the ECNS and a Smagorinsky constant of 0.12, and three different grid resolutions. *Bottom-left*: the ratio of the simulated value of the energy at a given wavenumber to the experimentally obtained value at the same wavenumber

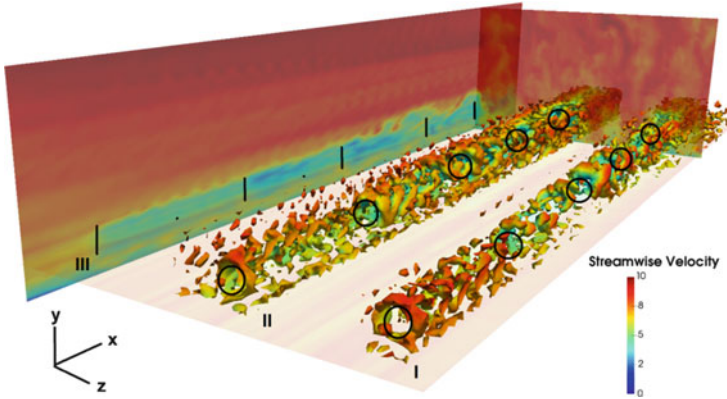


Fig. 20.6 Isosurfaces of Q-Criterion coloured by streamwise velocity in the wake of turbines on a simple wind farm. The ABL is neutral and runs through a wind farm with 15 turbines

20.6.3 Validation

The code with the chosen value of the Smagorinsky constant was validated against two test-cases.

- The simulation of an actuator disk's wake validated against particle image velocimetry measurements in the wake of a porous disc within a wind tunnel, designed to emulate the actuator disk concept (Lignarolo et al. 2014).
- The simulation of a neutral-ABL with the ECNS-Smagorinsky model, to obtain the correct velocity profile and turbulence statistics (Meyers 2011).

The value of the Smagorinsky constant is fit for either case; as a result, we are able to simulate the combination of the actuator disk method and the neutral atmospheric boundary layer (Fig. 20.6).

20.7 Case Study: EWTW

We use the validated ECNS-Smagorinsky LES code to simulate the turbines at the ECN Wind Turbine Test-Site Wieringermeer (EWTW) (Bot 2015). It has five turbines of diameter $D = 80$ m, separated in the streamwise direction by 305 m or $3.812D$. We simulate the turbines with an inflow velocity of 8 m s^{-1} at hub-height

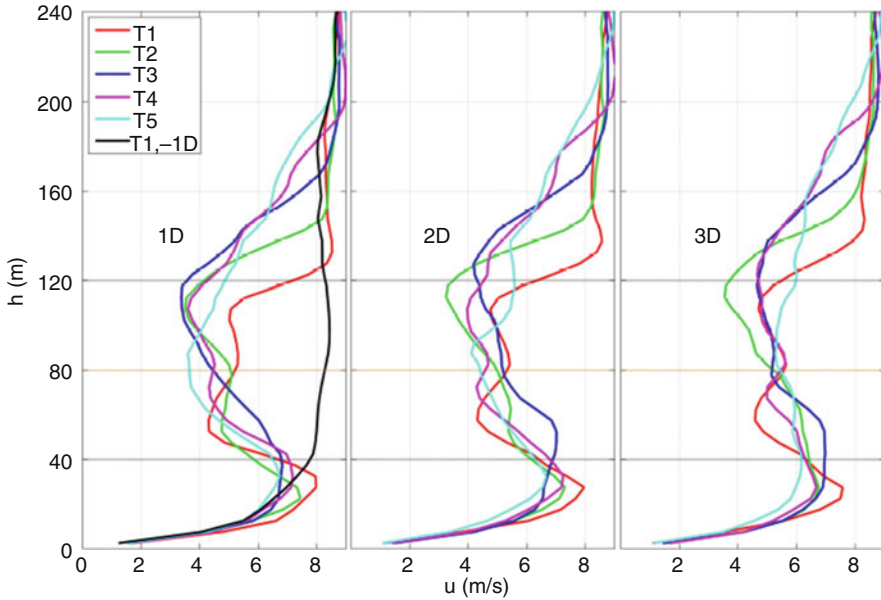


Fig. 20.7 Profiles of streamwise wake velocity behind the turbines at the EWTW

and a thrust coefficient of 0.789. We do not have ample experimental data to validate the ECNS, however, we do notice trends in the prediction of the wake velocity and turbulence intensity that are relevant to wake-turbine interaction across a row of turbines.

Figures 20.7 and 20.8 show the variation in velocity and turbulence intensity, respectively, with the vertical distance from the ground, behind 5 turbines, T1 to T5, at three downstream distances, 1D, 2D and 3D. In the leftmost plot within Figs. 20.7 and 20.8, the inflow profile has also been plotted (in black) at 1D before the first turbine, T1, or -1D. One notices trends similar to those explained in Sect. 20.4, regarding the recovery of velocity deficit, which is maximum behind the first turbine. However, the velocity recovers more rapidly behind the downstream turbines, as the turbulence intensity develops and reaches a fixed value, which aids the recovery of wake velocity.

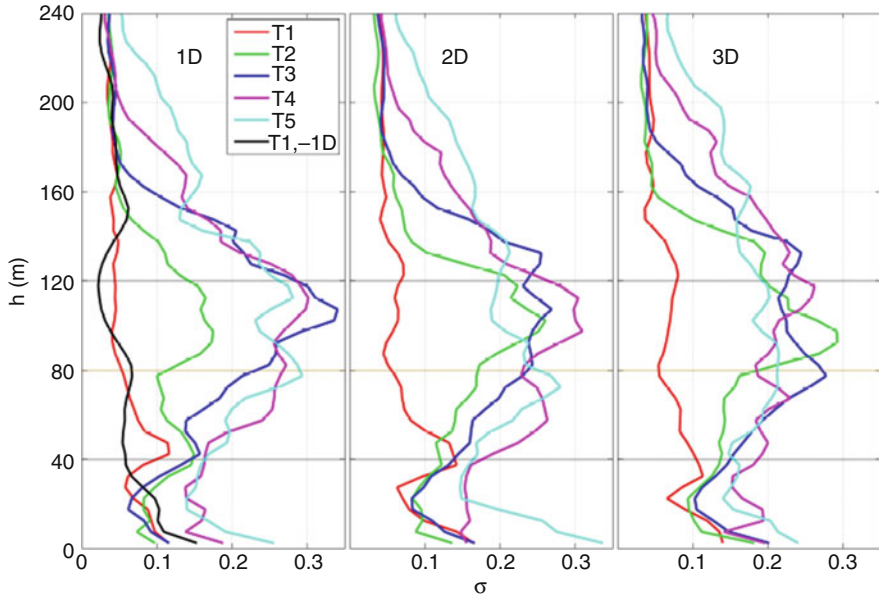


Fig. 20.8 Profiles of turbulence intensity behind the turbines at the EWTW

20.8 Conclusions and Recommendations

Based on the research we conclude the following:

- EC time integration is beneficial for averting numerical dissipation, which can lead the spurious decay of energy during wind farm simulations, and eventually, producing a wrong estimate of power generation. However, a non-EC time integration scheme can also guarantee minimal numerical dissipation at a small time step, at significantly lower computational costs.
- EC spatial discretisation helps tune the Smagorinsky model for a range of grid resolutions owing to the absence of numerical dissipation, which varies with grid resolution and must be accounted for while tuning.
- The Smagorinsky constant obtained through tuning the model for decaying isotropic homogeneous turbulence, can be used to simulate a neutral-ABL and the wake of an actuator disk and therefore, by extension, the flow through a wind farm.

For research in the future, we recommend the following:

- Developing an optimised method to using the EC time integration schemes more efficiently. Although non-EC schemes are a fine alternative, they are restricted by a stability criterion that prevents the use of local grid refinement. Such, refinement can help gain insight into critical phenomena in the wake and the

ABL as a whole. Using an EC time scheme that is implicit, will not only remove the restriction on grid refinement but also avert numerical dissipation.

- Simple schemes such as the central difference scheme in OpenFOAM can readily be used for wind farm aerodynamics, instead of developing new computational methods.

Open Access This chapter is distributed under the terms of the Creative Commons Attribution-NonCommercial 4.0 International License (<http://creativecommons.org/licenses/by-nc/4.0/>), which permits any noncommercial use, duplication, adaptation, distribution and reproduction in any medium or format, as long as you give appropriate credit to the original author(s) and the source, provide a link to the Creative Commons license and indicate if changes were made.

The images or other third party material in this chapter are included in the work's Creative Commons license, unless indicated otherwise in the credit line; if such material is not included in the work's Creative Commons license and the respective action is not permitted by statutory regulation, users will need to obtain permission from the license holder to duplicate, adapt or reproduce the material.

References

- Barthelmie RJ, Frandsen ST, Hansen K et al (2009) Modelling the impact of Wakes on Power Output at Nysted and Horns. Paper presented at the EWEC 2009, European wind energy conference and exhibition, Marseille 16–19 March 2009
- Bot ETG (2015) FarmFlow validation against full scale wind farms, Technical Report ECN-E-15-045. In: Energy research Centre of the Netherlands publications. Available via ECN. <https://www.ecn.nl/publications/PdfFetch.aspx?nr=ECN-E--15-045>. Accessed 12 Apr 2016
- Calaf M, Meneveau C, Meyers J (2010) Large Eddy Simulation study of fully developed wind-turbine array boundary layers. *Phys Fluids*. doi:[10.1063/1.3291077](https://doi.org/10.1063/1.3291077)
- Chamorro LP, Porté-Agel F (2011) Turbulent flow inside and above a wind farm: a wind tunnel study. *Energies* 4:1916–1936
- Comté-Bellot G, Corrsin S (1971) Simple Eulerian time correlation of full and narrow band velocity signals in grid generated isotropic turbulence. *J Fluid Mech* 48:272–337
- Ivanell SSA (2009) Numerical computations of wind turbine wakes. In: Technical reports from the Royal Institute of Technology, Linné Flow Centre, Department of Mechanics, Stockholm. Available via KTH. <https://sverigesradio.se/diverse/appdata/isidor/files/3345/10845.pdf>. Accessed 12 Apr 2016
- Lignarolo L, Ragni D, Krishnaswami C et al (2014) Experimental analysis of a horizontal axis wind-turbine model. *Renew Energ* 70:31–46
- Mehta D, van Zuijlen AH, Koren B et al (2014) LES of wind farm aerodynamics: a review. *J Wind Eng Ind Aerod* 133:1–17
- Meyers J (2011) Error-landscape assessment of large-eddy simulations: a review of the methodology. *J Sci Comput* 49:65–77
- Panofsky H, Dutton J (1984) Atmospheric turbulence: models and methods for engineering applications. Wiley, New York
- Perić M, Ferziger J (2002) Computational methods for fluid dynamics. Springer, Berlin
- Pope SB (2000) Turbulent flows. Cambridge University Press, Cambridge
- Sanderse B (2013) Energy conserving discretisation methods for the incompressible Navier-Stokes equations: application to the simulation of wind-turbine wakes. Dissertation, Eindhoven University of Technology
- Stevens RJAM, Gayme DF, Meneveau C (2013) Effect of turbine alignment on the average power output of wind farm. In: Abstracts of the ICOWES 2013 international conference on aerodynamics of offshore wind energy systems and wakes, Lyngby, 17–19 June 2013
- Tennekes H, Lumley JL (1972) A first course in turbulence. MIT Press, London